Electric Power Systems Research 212 (2022) 108547

Contents lists available at ScienceDirect

Electric Power Systems Research

journal homepage: www.elsevier.com/locate/epsr

Model-less robust voltage control in active distribution networks using sensitivity coefficients estimated from measurements

Rahul Gupta [a,*], Fabrizio Sossan [b], Mario Paolone [a]

[a] Distributed Electrical Systems Laboratory, EPFL, Switzerland
[b] PERSEE, Mines ParisTech, France

ARTICLE INFO

Keywords:
Data-driven control
Inference
Model-less
Robust voltage control
Recursive least squares
Least squares

ABSTRACT

Measurement-rich power distribution networks may enable distribution system operators (DSOs) to adopt model-less and measurement-based monitoring and control of distributed energy resources (DERs) for mitigating grid issues such as over/under voltages and lines congestions. However, measurement-based monitoring and control applications may lead to inaccurate control decisions due to measurement errors. In particular, estimation models relying on regression-based schemes result in significant errors in the estimates (e.g., nodal voltages) especially for measurement devices with high Instrument Transformer (IT) classes. The consequences are detrimental to control performance since this may lead to infeasible decisions. This work proposes a model-less robust voltage control accounting for the uncertainties of measurement-based estimated voltage sensitivity coefficients. The coefficients and their uncertainties are obtained using a recursive least squares (RLS)-based online estimation, updated whenever new measurements are available. This formulation is applied to control distributed controllable photovoltaic (PV) generation in a distribution network to restrict the voltage within prescribed limits. The proposed scheme is validated by simulating a CIGRE low-voltage network interfacing multiple controllable PV plants.

1. Introduction

Distribution system operators (DSOs) are required to operate their networks ensuring the quality of supply (QoS) while respecting the network's physical limits [1–3]. However, the progressive installation of decentralized generation such as Photo-voltaic (PV) units in distribution networks is causing power quality issues such as voltage violations as well as congestions in both lines and transformers. Conventional methods tackle these problems by passive curtailments of loads/generations, generation tripping, shunt capacitor banks and, eventually expensive network reinforcement. Authors in [4] lay out the potential ways to manage the electricity supply in modern power systems with a high amount of renewable generations. In order to limit expensive grid reinforcement programs, DSOs may need to adopt intelligent control schemes of distributed energy resources (DERs) (e.g., [5, 6]) for the safe operation of their grids.

Voltage control is one of the widely acknowledged control schemes to be adopted and improved in power distribution networks. Conventional voltage controls are based on volt-var schemes, where only the reactive power is controlled to regulate nodal voltages. However, as shown in [7], the sole reactive power control might not be enough especially for grids with high R/X ratio of branches longitudinal impedances, the control of both active and reactive powers may be needed. In the literature, this type of control can be broadly categorized into two kinds. The first relies on the network model (network topology, branch, and shunt parameters). These methods are also referred to as model-based methods. For example, in [8,9], it is proposed a distributed control of PV inverters for regulating the nodal voltage magnitudes in a distribution grid where the grid constraints are modeled using the admittance matrix of the network. However, in many cases, the network parameters are either unavailable, partially missing, or outdated. Thanks to the increasing adoption of monitoring systems such as smart meters in present distribution networks, measurement-based/data-driven/model-less control schemes can be an alternative. This leads to the second kind of voltage control scheme often referred to as measurement-based schemes [7,10–13]. These schemes are used for real-time voltage control where the network model is inferred from the measurements (e.g. [14]). However, in all the reported model-less and measurement-based methods, the control or the estimation problem does not consider uncertainty on the estimated grid models (e.g., estimated sensitivity coefficients) and may result in wrong control decisions. The uncertainty on the measurement-based estimated model comes from the measurement noise of the instrument transformers

* Corresponding author.
E-mail addresses: rahul.gupta@epfl.ch (R. Gupta), fabrizio.sossan@mines-paristech.fr (F. Sossan), mario.paolone@epfl.ch (M. Paolone).

https://doi.org/10.1016/j.epsr.2022.108547
Received 4 October 2021; Received in revised form 14 April 2022; Accepted 2 July 2022
Available online 20 July 2022

(ITs). As reported in [15,16], the estimated sensitivity coefficients suffer high biases due to measurement noise and fluctuating values due to collinearity in the measured data set.

In this work, we propose a model-less robust voltage control that accounts for the uncertainty on the measurement-based estimated sensitivity coefficients ensuring safe and reliable operation of the distribution grid. The work comprises the estimation of the sensitivity coefficients and their uncertainties and use them to provide robustness against the inaccuracies of measurement-based estimated grid models [17]. The proposed voltage control problem consists of two stages: in the first stage, an estimation problem is solved to estimate the voltage sensitivity coefficients and their uncertainties. In the second stage, we solve a robust voltage control problem accounting for the uncertainties on the estimated coefficients. Overall, the contributions of this paper are as follows:

- we investigate the effect of uncertainties of the voltage sensitivity coefficients estimates adopted in model-less voltage control of distributed PV generations in a power distribution systems. We show how this may result in voltage violations;
- we formulate a robust voltage control problem using the measurement-based estimated sensitivity coefficients and their uncertainties;
- we present a performance comparison of different estimation techniques of measurement-based estimations of sensitivity coefficients for the proposed robust control.

The performance assessment is carried out on the CIGRE LV [2] network interfacing multiple controllable PV units. First, we evaluate different techniques for estimating the sensitivity coefficients and their uncertainties, then the dominant method is chosen to be coupled with a robust control scheme. To show the effectiveness of the proposed robust formulation, we compare it with non-robust voltage control case when uncertainties are not considered. The performance is also benchmarked against model-based control.

The paper is organized as follows. Section 2 presents the model-less robust control framework, Section 3 presents different estimation methods for the estimation of the sensitivity coefficients, Section 4 presents the voltage control problem and its robust reformulation. Section 5 describes the considered test-case and respective estimation and control results, and finally Section 6 concludes the work.

2. Proposed model-less robust voltage control framework

Let us consider a power distribution network equipped with measurement devices capable of providing high throughput measurements on nodal voltage magnitudes and active/reactive powers. Let N_b be the number of non-slack buses and the set $\mathcal{N}^b = \{1, \dots, N_b\}$ defining the bus indices. The distribution network hosts multiple DERs (for example, PV generation units) that can be controlled to provide active and reactive power support to the grid. The objective is to control DERs in real-time or quasi-real-time such that grid constraints are always respected. The parameters and topology of the network are not known, so model-based controls could not be implemented. The control scheme solely relies on a model-less scheme, where the grid constraints (such as nodal voltages, lines, and transformer power flows) are accounted by models estimated from measurements. Although the model-less framework is generic and can be applied for various control schemes, this work focuses on the voltage control problem where the DERs are controlled in real-time to avoid or mitigate voltage problems.

The model-less control framework consists of two stages: in the first one, measurements on voltages and active/reactive power magnitudes are used to estimate the voltage sensitivity coefficients; these are then used by the voltage control stage. We compute the uncertainties of the estimated sensitivity coefficients in order to formulate a robust voltage control problem. The uncertainties of the estimates are inferred using the inverse of the Fischer information matrix [18]. Fig. 1 shows the flow diagram illustrating the proposed two-stage scheme for the robust model-less control framework. The first stage (on the left) is composed of a measurement-based estimation loop that stores nodal voltage magnitudes, active and reactive power measurements and estimates the voltage sensitivity coefficients and their uncertainties. Then, the block on the right solves the constrained optimization problem for controlling DERs to mitigate the voltage problems in the network. They are described as follows.

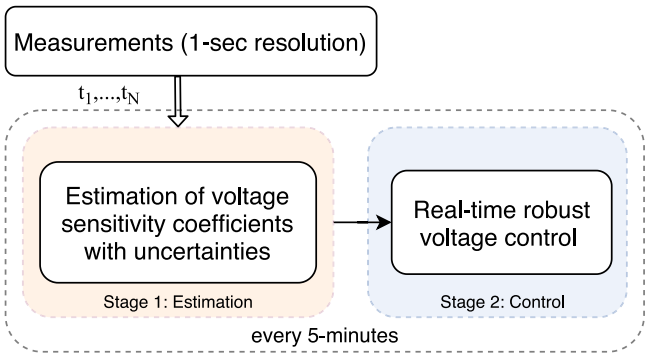

Fig. 1. Model-less/measurement-based robust voltage control framework.

3. Measurement-based estimation of voltage sensitivity coefficients and their uncertainties

The voltage sensitivity coefficient of the ith node with respect to absorbed/injected power at node j is defined as

$$K_{ij}^P = \frac{\partial V_i}{\partial P_j};\ K_{ij}^Q = \frac{\partial V_i}{\partial Q_j} \tag{1}$$

where, K_{ij}^P K_{ij}^Q are the sensitivity coefficients of the nodal voltage magnitudes V_i of node i with respect to the active and reactive power injections P_j, Q_j of node j. Using the measurements on voltage magnitudes and active/reactive power injections, these sensitivity coefficients are estimated. We assume following hypothesis to hold true.

Hypothesis 1. The DSO does not know the network parameters, and the topology, and the system state.

Hypothesis 2. The distribution network is equipped with measurements units providing the operator with the measurements of voltage magnitudes, and active and reactive power injections at regular time intervals. The metering devices are aligned with a network time protocol (e.g. NTP [19]).

Hypothesis 3. The sensitivity coefficients remain unchanged over a time window[1] (5 min in this case) which is used to collect adequate number of measurements in the estimation problem.

Hypothesis 4. The system is in steady-state, and the power injection is subject to small dynamics that the first-order Taylor approximations can represent with enough accuracy [9,20].

Hypothesis 5. The magnitude error from the ITs and voltmeter measurements is Gaussian. It behaves according to the standards and they do not have a bias [21,22].

[1] We assume that there is no significant change in the network's operating conditions, such as topology or step change of the load/generation. If it happens, the fixed time window could be replaced by a variable time window where sensitivity coefficients are re-estimated.

The objective is to estimate the voltage sensitivity coefficients and their uncertainties by using the measurements of nodal voltage magnitudes, active and reactive powers. The method is described as follows.

3.1. Estimation model

Using the coefficient definition in (1) and Taylor's first-order approximation, the magnitude deviation of the nodal voltages at time t_k for node i can be written as

$$\underbrace{\Delta V_{i,t_k}}_{\gamma_{t_k}} \approx \underbrace{[\Delta \mathbf{P}_{t_k} \ \Delta \mathbf{Q}_{t_k}]}_{h_{t_k}} \underbrace{\begin{bmatrix} \mathbf{K}^P_{i,t_k} \\ \mathbf{K}^Q_{i,t_k} \end{bmatrix}}_{\mathbf{X}} \tag{2}$$

where $V_{i,t_k} - V_{i,t_{k-1}} = \Delta V_{i,t_k} \in \mathbb{R}$ is the deviation of nodal voltage magnitude of ith node, vectors $\mathbf{P}_{t_k} - \mathbf{P}_{t_{k-1}} = \Delta \mathbf{P}_{t_k}, \mathbf{Q}_{t_k} - \mathbf{Q}_{t_{k-1}} = \Delta \mathbf{Q}_{t_k} \in \mathbb{R}^{N_b}$ include deviations of active and reactive powers of all the nodes from timestep t_{k-1} to t_k. The vectors $\mathbf{K}^P_{i,t_k}, \mathbf{K}^Q_{i,t_k} \in \mathbb{R}^{N_b}$ include voltage sensitivity coefficients of ith node with respect injections of nodes $j \in \mathcal{N}^b$. It should be noted that the approximation in (2) of the power-flow equations involves two errors: (i) the linearization and (ii) the measurement noise. In this work, we assume that the linearization error is negligible compared to the one due to the measurement noise. This assumption is reasonable if the state of the system is slow varying and the control is acting in quasi real-time. Assuming that we have measurements for time $t = t_1 \dots, t_N$ and coefficients do not change for N timesteps (Hypothesis 3), Eq. (2) can be written as

$$\mathbf{\Gamma} \approx \mathbf{H}\mathbf{X} \tag{3}$$

where, $\mathbf{\Gamma} \in \mathbb{R}^N = [\gamma_{t_1} \gamma_{t_2} \dots \gamma_{t_N}]^T$, $\mathbf{H} \in \mathbb{R}^{N \times 2N_b} = [h_{t_1} h_{t_2} \dots h_{t_N}]^T$ and $\mathbf{X} \in R^{2N_b}$ includes $\mathbf{K}^P_{i,t_k}$ and $\mathbf{K}^Q_{i,t_k}$. Eq. (3) can be re-written assuming noise model to be white Gaussian (Hypothesis 5).

$$\mathbf{\Gamma} = \mathbf{H}\mathbf{X} + \mathcal{W} \qquad \mathcal{W} \in \mathcal{N}(\mathbf{0}, \Sigma), \tag{4}$$

Σ refers to the noise covariance matrix.

3.2. Estimation technique

The linear model in (4) is typically solved for $\mathbf{X}$ by minimizing the norm-2 difference of the residual, known as Least-Squares (LS). However, the LS method does not perform well in case of low excitation (nodal power injections are low) and suffers from the problem of multicollinearity (power injections at different nodes are very similar) [12,16]. Also, the sensitivity coefficients vary as a function of network's states so, it is necessary to use the most recent estimates during a real-time control. Thus, an online estimation scheme was used in [12,13] that used recursive least square (RLS)-based estimation coupled with an offline LS. In this work, we use this scheme to estimate the sensitivity coefficients. Fig. 2 shows the dataflow of the estimation process. First, the LS is used to get a rough estimates of the coefficients. Then, the RLS is used to refine the LS estimates by using the latest information on the voltage and power measurements. The LS is solved off-line using a large number of historical measurements. The RLS problem is solved at each time step using recent measurements where the LS estimation is used to initialize the RLS. Both the processes are described next.

3.2.1. Offline LS

Offline LS problem is formulated as

$$\hat{\mathbf{X}} = \min_{\mathbf{X}} \|\mathbf{\Gamma} - \mathbf{H}\mathbf{X}\|_2 + \lambda \mathbf{X}^T\mathbf{X} \tag{5}$$

where λ is a positive number that serves as a regularization parameter and is used to avoid ill-conditioned information matrix (i.e., in case of multi-collinearity nodal injections). The closed-form solution of (5) is obtained in view of its quadratic and unconstrained nature as,

$$\hat{\mathbf{X}}_{t_0} = (\mathbf{H}^T\mathbf{H} + \lambda \mathbf{I})^{-1}\mathbf{H}^T\mathbf{\Gamma} = (\mathbf{R}_{t_0} + \lambda \mathbf{I})\mathbf{H}^T\mathbf{\Gamma} \tag{6}$$

where $\mathbf{I}$ is the identity matrix. The covariance matrix is defined as inverse of the information matrix, i.e. $\mathbf{P}^{\text{cov}}_{t_0} = \mathbf{R}^{-1}_{t_0}$.

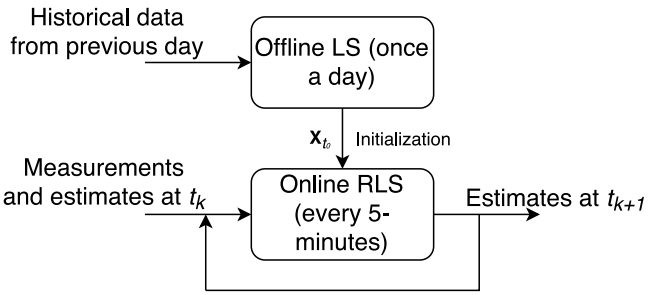

Fig. 2. Flow diagram for two-stage estimation of sensitivity coefficients.

3.2.2. Online RLS

In this scheme, an online recursive estimation is performed using the most recent measurements. It utilizes the estimates from the previous time step and measurements at the current time step. RLS updates the estimates whenever the new data is available. LS solution in (6) is used to initialize the RLS stage. The use of exponential forgetting factor applied to the observations is advised to give less importance to previous measurements [23]. The forgetting factor $0 < \mu \leq 1$ is reflected in the covariance matrix update.

$$\mathbf{R}_{t_k} = \mu \mathbf{R}_{t_{k-1}} + h^T_{t_k} h_{t_k} \tag{7}$$

This results in the following iterative updates.

$$e_{t_k} = \gamma_{t_k} - h_{t_k}\hat{\mathbf{X}}_{t_{k-1}} \tag{8a}$$

$$\hat{\mathbf{X}}_{t_k} = \hat{\mathbf{X}}_{t_{k-1}} + \mathcal{L}_{t_k} e_{t_k} \tag{8b}$$

$$\mathcal{L}_{t_k} = \frac{\mathbf{P}^{\text{cov}}_{t_{k-1}} h^T_{t_k}}{\mu + h_{t_k}\mathbf{P}^{\text{cov}}_{t_{k-1}} h^T_{t_k}} \tag{8c}$$

$$\mathbf{P}^{\text{cov}}_{t_k} = (\mathbf{I} - \mathcal{L}_{t_k} h_{t_k})\mathbf{P}^{\text{cov}}_{t_{k-1}}/\mu \tag{8d}$$

where, $\mathcal{L}$ is the estimated gain and e the residual. In the following, this scheme is referred to as RLS-F.

As reported in [23,24], the RLS-F scheme suffers from the windup problem of the covariance matrix . It may lead to very large covariances resulting in large estimates variances. Multiple schemes are proposed in the literature to solve this problem. They are briefly described next.

3.2.2.1. Constant-trace scheme (RLS-CT). In [25], it is discussed how to limit the windup problem of the co-variance matrix by setting an upper bound on the trace sum of the covariance matrix and adding an identity matrix $\mathbf{I}$. The scheme uses two different factors c_1 and c_2 such that $c_1/c_2 = 10e3$; $h_{t_k} h^T_{t_k} c_1 \gg 1$. The covariance matrix is modified as:

$$\mathbf{P}^{\text{cov}}_{t_k} = c_1 \mathbf{P}^{\text{cov}}_{t_k}/\text{trace}(\mathbf{P}^{\text{cov}}_{t_k}) + c_2\mathbf{I} \tag{9}$$

3.2.2.2. Selective forgetting (RLS-SF). In [23] it is proposed to use selective forgetting factor, i.e., to use different forgetting factors for different eigenvalues of the covariance matrix. These forgetting factors are computed and updated iteratively to limit the windup problem of the covariance matrix. The gain and covariance matrix are updated as follows.

$$\mathcal{L}_{t_k} = \frac{\mathbf{P}^{\text{cov}}_{t_{k-1}} h^T_{t_k}}{1 + h_{t_k}\mathbf{P}^{\text{cov}}_{t_{k-1}} h^T_{t_k}} \tag{10a}$$

$$\mathbf{P}^{\text{cov}}_{t_k} = \sum_{i=1}^{2N_b} \frac{\tau_{i,t_k}}{\mu_i} u^T_{i,t_k} u_{i,t_k}. \tag{10b}$$

Here, u_{i,t_k} denotes the eigenvectors of $\mathbf{P}^{\text{cov}}_{t_k}$ in Eq. (8d) and τ_{i,t_k} the corresponding eigenvalues. It proposed to limit τ_{i,t_k} by a function f that keeps it within bounds $[\tau_{\min}\ \tau_{\max}]$:

$$\tau_{i,t_k} = f(\tau_{i,t_{k-1}}) \tag{10c}$$

$$f(x) = \begin{cases} x, & x > \tau_{\max} \\ \tau_{\min} + (1 - \tau_{\min}/\tau_{\max})x & x \le \tau_{\min} \end{cases} \tag{10d}$$

More information on the tuning of RLS-SF is in [23,25].

3.2.2.3. Directional forgetting (RLS-DF). In [26], [27] proposed directional forgetting algorithm where the matrix $\mathbf{R}$ is decomposed into two parts: the first part is fully propagated to the next time step, whereas the second part is propagated with a forgetting factor, μ. This method was first proposed in [26] and termed as "directional forgetting" as the two parts of the gain matrix are orthogonal to each other. Theoretical development supporting this algorithm is in [27]. The iterative updates of RLS-DF are

$$\mathcal{L}_{t_k} = \mathbf{P}^{\text{cov}}_{t_k} h^T_{t_k} \tag{11a}$$

$$\bar{\mathbf{P}}^{\text{cov}}_{t_{k-1}} = \mathbf{P}^{\text{cov}}_{t_{k-1}} + \frac{1-\mu}{\mu} \frac{h^T_{t_k} h_{t_k}}{h_{t_k} \mathbf{R}_{t_k} h^T_{t_k}} \tag{11b}$$

$$\mathbf{P}^{\text{cov}}_{t_k} = \bar{\mathbf{P}}^{\text{cov}}_{t_{k-1}} - \frac{\bar{\mathbf{P}}^{\text{cov}}_{t_{k-1}} h^T_{t_k} h_{t_k} \bar{\mathbf{P}}^{\text{cov}}_{t_{k-1}}}{1 + h_{t_k} \bar{\mathbf{P}}^{\text{cov}}_{t_{k-1}} h^T_{t_k}} \tag{11c}$$

$$\mathbf{R}_{t_k} = [\mathbf{I} - \mathbf{M}_{t_k}]\mathbf{R}_{t_{k-1}} + h^T_{t_k} h_{t_k} \tag{11d}$$

$$\mathbf{M}_{t_k} = (1-\mu) \frac{\mathbf{R}_{t_{k-1}} h^T_{t_k} h_{t_k}}{h_{t_k} \mathbf{R}_{t_{k-1}} h^T_{t_k}} \tag{11e}$$

The updates strategies for the covariance matrix directly affects the estimates and their uncertainties. The numerical performance of these schemes (i.e. RLS-F, RLS-CT, RLS-SF and RLS-DF) are assessed in the results section.

3.2.3. Estimation of uncertainties on sensitivity coefficients

In this work, we propose to account for the uncertainties of the estimated sensitivity coefficients to robustify the voltage control. The uncertainties are computed using the co-variance matrix given by

$$\sigma_{\mathbf{X}} = \sigma_r \sqrt{\text{diag}(\mathbf{P}^{\text{cov}})} \tag{12}$$

where σ_r is the estimated standard deviation of residuals inferred post-estimation. They are continuously updated during the RLS estimation stage. The uncertainty on the estimated coefficients are estimated to be $\pm 3\sigma_{\mathbf{X}}$ corresponding to the 99 % confidence interval.

4. Model-less robust voltage control problem

As previously mentioned, the proposed control uses the estimated coefficients and their uncertainties to formulate a robust voltage control problem. The robustification uses the technique from [28] where the robustness of a model-based voltage control was formulated against uncertainty in the resistances of the grid's branch impedances. In contrast, in this work we propose a measurement-based and mode-less way to define a robust voltage control.

In the following, first we introduce the non-robust voltage control problem (i.e., the uncertainty on the coefficients estimates are not accounted), then we present its robust counterpart.

4.1. Voltage control problem without considering uncertainty on the estimates (Non-robust)

Let us consider a distribution network connected with controllable PV generation units such that their active and reactive power injections can be controlled. Let the set $\mathcal{N}^{\text{pv}}$ includes indices of the PV units. The objective is to control active/reactive power injections $(P_{j,t_k}, Q_{j,t_k}, j \in \mathcal{N}^{\text{pv}})$ such that the nodal voltages are within the statutory bounds. Additionally, the local objective of the PV units is to minimize the curtailment of their active power generation and provide reactive power support. The problem we solve at time t_k is to minimize curtailments of PV plants:

$$\underset{P_{j,t_k}, Q_{j,t_k}, \forall j \in \mathcal{N}^b}{\text{minimize}} \sum_{j \in \mathcal{N}^{\text{pv}}} \left\{ (P_{j,t_k} - \hat{P}_{j,t_k})^2 + (Q_{j,t_k})^2 \right\} \tag{13a}$$

subject to the constraint on the PV generation limited by short-term MPP forecast $\hat{P}_{j,t_k}$,

$$0 \le P_{j,t_k} \le \hat{P}_{j,t_k} \qquad j \in \mathcal{N}^{\text{pv}} \tag{13b}$$

the capability constraint of the converter rating $S^{\max}_j$,

$$0 \le (P_{j,t_k})^2 + (Q_{j,t_k})^2 \le (S^{\max}_j)^2 \qquad j \in \mathcal{N}^{\text{pv}}, \tag{13c}$$

and the minimum power factor constraint

$$Q_{j,t_k} \le P_{j,t_k} \zeta \qquad j \in \mathcal{N}^{\text{pv}} \tag{13d}$$

$$-Q_{j,t_k} \le P_{j,t_k} \zeta \qquad j \in \mathcal{N}^{\text{pv}}. \tag{13e}$$

Here, $\zeta = \sqrt{(1 - \text{PF}^2_{\min})/\text{PF}^2_{\min}}$, being $\text{PF}_{\min}$ the minimum power-factor allowed for the PV operation of each PV plant. The final constraints are on the voltage magnitudes, which are bounded by $[V^{\min}, V^{\max}]$. The voltage magnitudes are modeled by the estimated voltage sensitivity coefficients as

$$V^{\min} \le V_{i,t_{k-1}} + \hat{\mathbf{K}}^P_{i,t_{k-1}} \Delta \mathbf{P}_{t_k} + \hat{\mathbf{K}}^Q_{i,t_{k-1}} \Delta \mathbf{Q}_{t_k} \le V^{\max} \quad \forall i \in \mathcal{N}^b \tag{13f}$$

The voltage sensitivity coefficients, $\hat{\mathbf{K}}^P_{i,t_{k-1}}, \hat{\mathbf{K}}^Q_{i,t_{k-1}}$, are estimated online using one of the estimation scheme described in Section 3 utilizing latest measurements on voltages and power magnitudes.

As described earlier, the non-robust problem in (13) does not account for the uncertainty on the estimates caused by measurement noise which might result in inaccurate control decisions leading to voltage violations.

4.2. Robust voltage control problem

We here illustrate the robust voltage control by accounting for the uncertainty on the measurement-based estimated voltage sensitivity coefficients. The robust counterpart of (13) can be formulated by adding following constraints to (13)

$$\mathbf{K}^P_{i,t_k} \in [\hat{\mathbf{K}}^P_{i,t_k} - \Delta \mathbf{K}^P_{i,t_k},\ \hat{\mathbf{K}}^P_{i,t_k} + \Delta \mathbf{K}^P_{i,t_k}] \qquad \forall i \in \mathcal{N}^b \tag{13g}$$

$$\mathbf{K}^Q_{i,t_k} \in [\hat{\mathbf{K}}^Q_{i,t_k} - \Delta \mathbf{K}^Q_{i,t_k},\ \hat{\mathbf{K}}^Q_{i,t_k} + \Delta \mathbf{K}^Q_{i,t_k}] \qquad \forall i \in \mathcal{N}^b. \tag{13h}$$

Here, $\Delta \mathbf{K}^P_{i,t_k}, \Delta \mathbf{K}^Q_{i,t_k}$ be the estimated uncertainty on $\hat{\mathbf{K}}^P_{i,t_k}, \hat{\mathbf{K}}^Q_{i,t_k}$. As known, accounting for the interval constraints makes the problem non-tractable in its original form. Thus, it is reformulated using the technique proposed in [28,29] summarized hereafter.

We introduce auxiliary variables $z_i, g_{ij}, y^p_j, y^q_j, j \in \mathcal{N}^{\text{pv}}, i \in \mathcal{N}^b$. We also introduce a parameter $\Omega_i \in [0, |\mathcal{N}^{\text{pv}}|]$ which provides a trade-off between the robustness and conservativeness of the solution as described in [28]. Considering these auxiliary variables and following the robust quadratic program with linear constraints in [29], the robust counterpart of the problem can be formulated as

$$\underset{P_{j,t_k}, Q_{j,t_k}, \forall j \in \mathcal{N}^b}{\text{minimize}} \sum_{j \in \mathcal{N}^{\text{pv}}} \left\{ (P_{j,t_k} - \hat{P}_{j,t_k})^2 + (Q_{j,t_k})^2 \right\} \tag{14a}$$

subject to:

(13b), (13c), (13d), (13e). (14b)

With the help of the auxiliary variables, the constraints on the nodal voltages are reformulated as follows.

$$V_{i,t_{k-1}} + \hat{\mathbf{K}}^P_{i,t_{k-1}} \Delta \mathbf{P}_{t_k} + \hat{\mathbf{K}}^Q_{i,t_{k-1}} \Delta \mathbf{Q}_{t_k} + z_i \Omega_i + \sum_{j \in \mathcal{N}^{\text{pv}}} g_{ij} \le V^{\max} \quad \forall i \in \mathcal{N}^b \tag{14c}$$

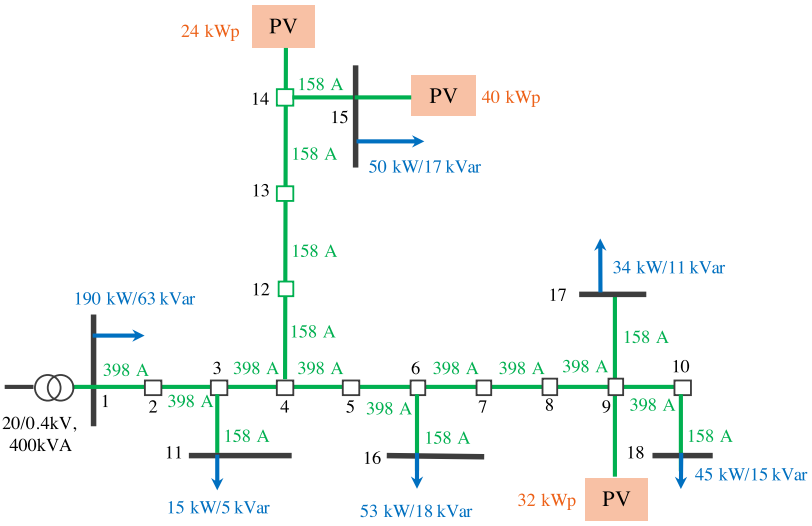

Fig. 3. Topology of the CIGRE low-voltage system with distributed PV units.

$$V_{i,t_{k-1}} + \hat{\mathbf{K}}^{P}_{i,t_{k-1}} \Delta \mathbf{P}_{t_k} + \hat{\mathbf{K}}^{Q}_{i,t_{k-1}} \Delta \mathbf{Q}_{t_k} - z_i \Omega_i - \sum_{j \in \mathcal{N}^{\text{pv}}} g_{ij} \geq V^{\min} \quad \forall i \in \mathcal{N}^b \tag{14d}$$

$$-y^p_j \leq \Delta P_{j,t_k} \leq y^p_j \qquad \forall j \in \mathcal{N}^{\text{pv}} \tag{14e}$$

$$-y^q_j \leq \Delta Q_{j,t_k} \leq y^q_j \qquad \forall j \in \mathcal{N}^{\text{pv}} \tag{14f}$$

$$z_i + g_{ij} \geq \Delta K^P_{ij,t_k} y^p_j \qquad i \in \mathcal{N}^b, j \in \mathcal{N}^{\text{pv}} \tag{14g}$$

$$z_i + g_{ij} \geq \Delta K^Q_{ij,t_k} y^p_j \qquad i \in \mathcal{N}^b, j \in \mathcal{N}^{\text{pv}} \tag{14h}$$

$$y^p_j, y^q_j, z_i, g_{ij} \geq 0 \qquad i \in \mathcal{N}^b, j \in \mathcal{N}^{\text{pv}}. \tag{14i}$$

The robust problem in (14) has a quadratic objective and linear constraints, hence it is convex and can be efficiently solved with any off-the-shelf solvers.

5. Simulation and results

5.1. Test-case and input data

For the validation of the measurement-based estimation and model-less control scheme and the corresponding performance evaluation, we consider a CIGRE benchmark low-voltage network [2]. The network is 20 kV/0.4 V, 400 kVA 3-ph balanced system as shown in Fig. 3. The nominal demands and the PV generation sites and sizes are also shown in the figure. In this case study, we assume reduced load condition such that the PV generation is causing over-voltages during the middle of the day. Fig. 4(a-b) shows the nodal active and reactive power injections. To obtain the ground-truth measurements of the voltage magnitudes and power injections, we carry simulated experiments performing load-flows by knowing the true admittance matrix of the grid. Then, the currents and voltages are corrupted with measurement noises characterized by the IT's specification described in [21,22]. This process is described in Algorithm 1. The algorithm introduces noise in polar coordinates (i.e., magnitudes and phase noise) on the voltage and currents, which is then used to compute the corrupted nodal active ($\tilde{\mathbf{P}}$) and reactive ($\tilde{\mathbf{Q}}$) power magnitudes. The specifications of the ITs are listed in Table 1.

5.2. Performance metrics

This section defines the metrics used in the performance assessment. The first metric is the classical root-mean-square-error (RMSE), defined as

$$\text{RMSE}(\hat{\mathbf{X}}) = \frac{\|\mathbf{X}^{\text{true}} - \hat{\mathbf{X}}\|_2}{\|\mathbf{X}^{\text{true}}\|_2}. \tag{15}$$

where, $\mathbf{X}^{\text{true}}, \hat{\mathbf{X}}$ are the true and estimated values of a generic quantity.

For the performance comparison on the estimation of the uncertainty intervals, we use metrics inspired by [30]: the first is the prediction interval coverage probability (PICP) that counts the number of instances realization falling within the uncertainty bounds for a given confidence interval α. It is

$$\text{PICP} = \frac{1}{N} \sum_{t_k=t_1}^{t_N} b_{t_k} \tag{16}$$

$$b_{t_k} = \begin{cases} 1 & \hat{K}^P_{ij,t_k} - \Delta K^P_{ij,t_k} \leq \hat{K}^P_{ij,t_k} \leq K^P_{ij,t_k} + \Delta K^P_{ij,t_k} \\ 0 & \text{otherwise.} \end{cases} \tag{17}$$

Table 1
Errors specifications for different class of Instrument Transformers Defined by [21,22].

IT class	Voltage transformers		Current transformers	
	Mag. error (σ^m) [%]	Phase error (σ^p) [rad.]	Mag. error (σ^m) [%]	Phase error (σ^p) [rad.]
0.2	0.2	3e−3	0.2	3e−3
0.5	0.5	6e−3	0.5	9e−3
1	1	12e−3	1	18e-3

Algorithm 1 Raw-data generation

Require: Admittance matrix: $\mathbf{Y}$, nodal power injections: $\mathbf{P}, \mathbf{Q}$
procedure GenData
  for $t_k = t_1 : t_N$ **do**
    $[\mathbf{V}(t_k), \mathbf{I}(t_k)] = \text{LoadFlow}(\mathbf{P}(t_k), \mathbf{Q}(t_k), \mathbf{Y})$
    $[\tilde{\mathbf{V}}(t_k), \tilde{\mathbf{I}}(t_k)] =$
    for $\beta = [\mathbf{V}(t_k), \mathbf{I}(t_k)]$ **do**
      $\delta^m = \mathcal{N}(0, \sigma^m|\beta|/3)$
      $|\beta| = |\beta| + \delta^m$
      $\delta^p = \mathcal{N}(0, \sigma^p/3)$
      $\arg(\beta) = \arg(\beta) + \delta^m$
      $\beta = |\beta|\exp(j\ \arg(\beta))$
    end for
    $\tilde{\mathbf{P}}(t_k) + j\tilde{\mathbf{Q}}(t_k) = \tilde{\mathbf{V}}(t_k)\tilde{\mathbf{I}}(t_k)^*$
  end for
end procedure

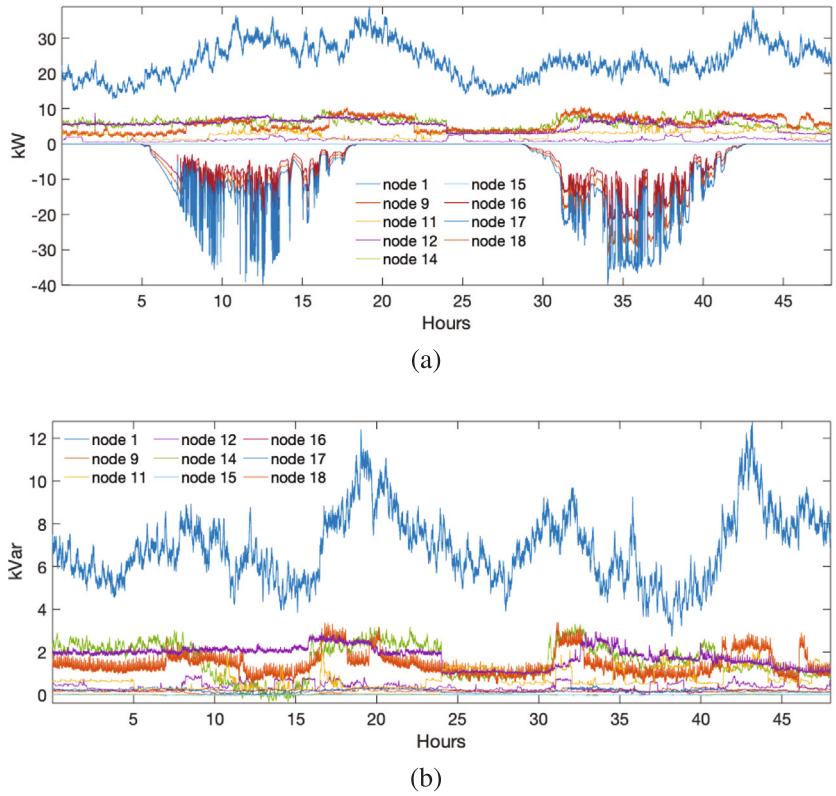

Fig. 4. (a) Nodal active (in kW) and (b) reactive (in kVar) power injections for non-zero injection nodes.

The second is the prediction interval normalized average width (PINAW):

$$\text{PINAW} = \frac{1}{N(K^P_{ij,\max})} \sum_{t_k=t_1}^{t_N} (2\Delta K^P_{ij,t_k}). \tag{18}$$

Being $K^P_{ij,\max}$ the maximum value of the coefficient in the series. The final metric is the coverage width-based criterion (CWC), which quantifies the trade-off between high PICP and small PINAW. It is

$$\text{CWC} = \text{PINAW}(1 + \eta(\text{PICP})e^{-\nu(\text{PICP}-\alpha)}), \tag{19}$$

$$\eta = \begin{cases} 0, & \text{PICP} \leq \alpha \\ 1, & \text{otherwise} \end{cases}. \tag{20}$$

The parameter ν can be set based on a tradeoff between the interval width penalization. We chose it to be $\nu = 50$. The considered confidence α is 99%.

5.3. Estimation results

We estimate $\mathbf{K}^P, \mathbf{K}^Q$ for the nodes where the controllable units (i.e., PV generation units) are connected. The estimation results using the measurements corresponding to IT 1.0 are presented below. The estimated coefficients are shown for the 2nd day with peak PV production during 32–42 h (potentially causing over-voltages). For performance comparison among different schemes, we report the estimations for LS, RLS-F, RLS-CT, RLS-SF, and RLS-DF as defined in Section 3.2. "LS" solves the LS algorithm and uses the measurements from last 5 min (sampled at 1-second, i.e., 30 samples) to estimate the sensitivity coefficients. For the methods based on the RLS, the first-day measurements (0–24 h) are used to compute initial estimates (offline-LS). Then, they are updated each 5-minutes with the last timestep measurements in a recursive way. The forgetting factor $\mu = 0.85$ is used in the simulations.

Figs. 5–9 shows the estimations and prediction intervals with confidence interval coverage of 99%. For the sake of brevity, we show only three coefficients which are $K^P_{15,15}, K^P_{14,8}, K^Q_{15,18}$ in Fig. 5–9(a), (b) and (c) respectively. The plots in red show the estimated coefficients, and the gray area their corresponding uncertainty. The black line shows the true coefficients.

As observed from the plot, LS fails in reliably estimating the coefficients and suffers from biases and large variances. The RLS-F exhibits large uncertainty on the estimates. This is due to the windup problem in the covariance matrix, as reported in [23]. RLS-CT, RLS-SF, and RLS-DF do fix the windup problem using the strategies described in Section 3.2. However, the RLS-CT fails to reliably estimate for the coefficient $K^Q_{15,18}$. RLS-SF and RLS-DF show similar performances. However, the former fails to cover the true coefficient during 32–34 h for $K^P_{15,15}$.

To have a proper comparison, we report the RMSE and the PICP-PINAW-CWC in Table 2 for the coefficient $K^P_{15,15}$ for the same duration (32–42 h) using different methods and with measurements characterized by other IT classes. From such a comparison, it can be observed that the RLS-DF performs the best with respect to all the metrics, i.e., it has the lowest RMSE and highest coverage. From Table 2, it can be observed that for all the estimation techniques, the RMSE increases for increasing measurement noise. The RLS-DF has full PICP coverage for all the IT classes, whereas the RLS-SF has slightly lower PICP for IT 0.5 and IT 1.0. From the comparison, it can be concluded that RLS-DF is the dominant estimation method.

5.4. Control results

In the following, we present the voltage control results. We control all three PV plants using the robust and non-robust approaches described in Section 4. The objective is to restrict the voltage magnitudes within the bounds 0.97–1.03 pu. We show the results only using the dominant estimation schemes i.e., RLS-SF and RLS-DF from the last analysis. In this setup, the previous day measurements (0–24 h) are used to compute initial estimates (offline-LS) for the RLS. Then, the online-RLS refines these estimates every 5 min using the last measurements. The latest estimated coefficients and their uncertainties are then

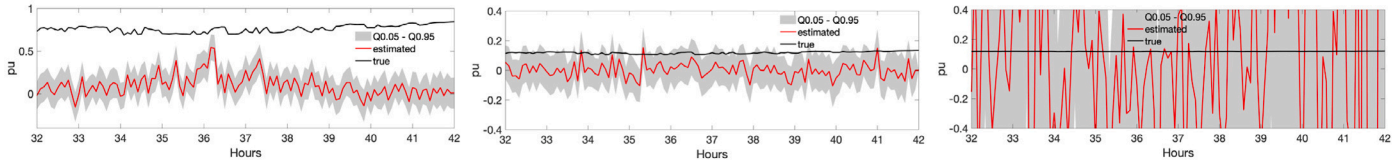

(a) $K^P_{15,15}$ (b) $K^P_{14,8}$ (c) $K^Q_{15,18}$

Fig. 5. Coefficients estimates and their uncertainty using the LS.

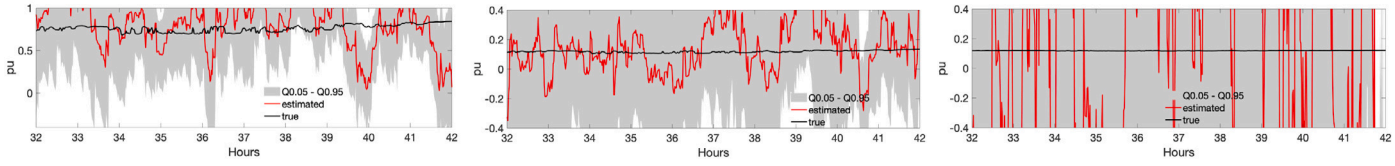

(a) $K^P_{15,15}$ (b) $K^P_{14,8}$ (c) $K^Q_{15,18}$

Fig. 6. Coefficients estimates and their uncertainty using the RLS-F.

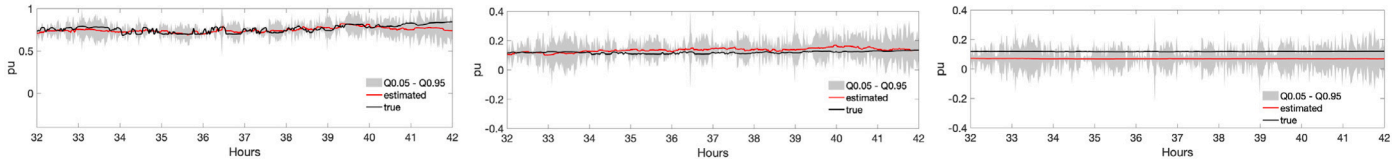

(a) $K^P_{15,15}$ (b) $K^P_{14,8}$ (c) $K^Q_{15,18}$

Fig. 7. Coefficients estimates and their uncertainty using the RLS-CT.

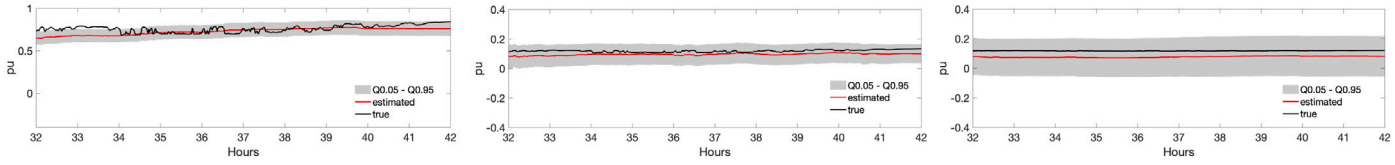

(a) $K^P_{15,15}$ (b) $K^P_{14,8}$ (c) $K^Q_{15,18}$

Fig. 8. Coefficients estimates and their uncertainty using the RLS-SF.

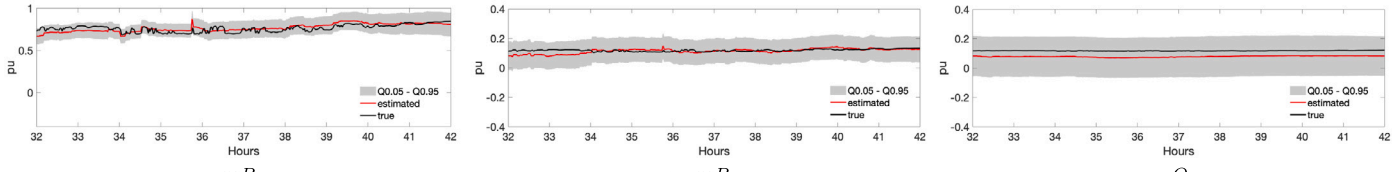

(a) $K^P_{15,15}$ (b) $K^P_{14,8}$ (c) $K^Q_{15,18}$

Fig. 9. Coefficients estimates and their uncertainty using the RLS-DF.

Table 2
Performance comparison of different estimation techniques for $K^P_{15,15}$ with different IT classes.

Method	IT 0.2		IT 0.5		IT 1.0	
	RMSE	PICP-PINAW-CWC	RMSE	PICP-PINAW-CWC	RMSE	PICP-PINAW-CWC
LS	0.89	0.14-0.36–0.41	0.94	0.03-0.35–0.37	0.98	0.04-0.41-0.43
RLS-F	0.46	0.99-1.05–1.85	0.39	0.93-1.45–2.70	0.43	0.86-1.32-2.38
RLS-CT	0.16	0.18-0.11–0.11	0.05	0.87-0.19–0.34	0.05	0.88-0.23-0.42
RLS-SF	0.05	1.00-0.42–0.42	0.07	0.83-0.19–0.35	0.06	0.89-0.18-0.33
RLS-DF	0.05	1.00-0.47–0.47	0.05	0.99-0.24–0.24	0.06	0.99-0.26-0.26

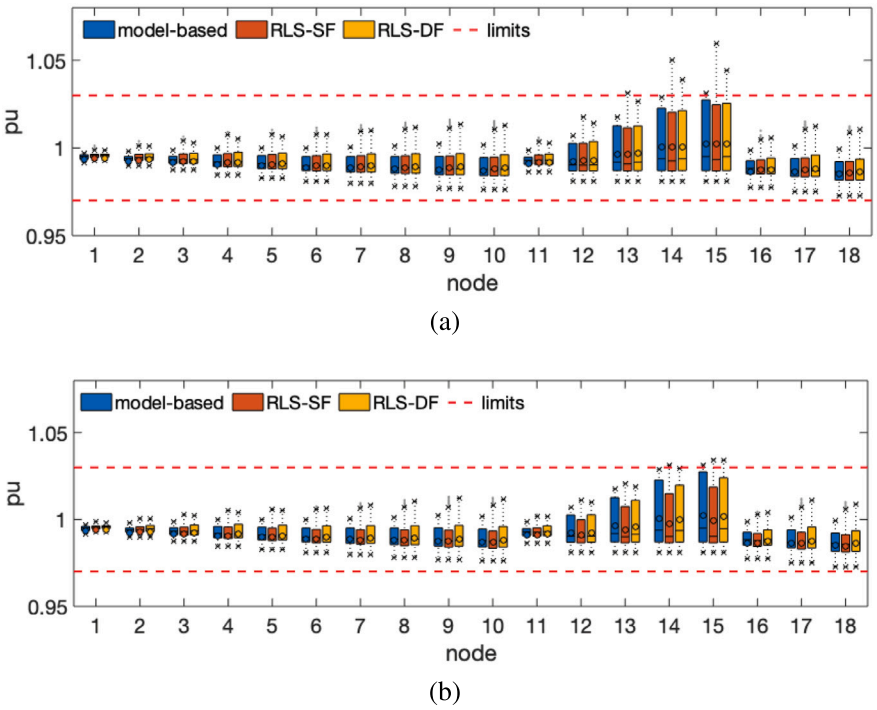

Fig. 10. Distribution of daily nodal voltage magnitudes using (a) non-robust and (b) robust voltage control.

Table 3
Performance comparison of different voltage control methods: maximum nodal voltage magnitude.

Method	IT 0.2		IT 0.5		IT 1.0	
	Non-robust	Robust	Non-robust	Robust	Non-robust	Robust
Model-based			1.031			
RLS-SF (model-less)	1.041	1.032	1.043	1.032	1.059	1.034
RLS-DF (model-less)	1.036	1.031	1.043	1.034	1.045	1.034

used for the voltage control. To compare the voltage violations produced by the different control schemes, the power set-points from these control schemes are fed to the non-linear AC power flow equations to obtain the actual nodal voltages.

5.4.1. Non-robust voltage control

Fig. 10(a) compares the daily boxplot post-control nodal voltage magnitudes for all the nodes using the non-robust control. The performance is also compared against *model-based* method, i.e., when the true sensitivity coefficients are known. As clear from the comparison, the non-robust control fails to restrict the voltage magnitudes of nodes 14 and 15 within imposed bounds by a large margin, irrespective of the estimation techniques. It should be noted that even the dominant estimation method (i.e., RLS-DF) fails to respect the upper voltage constraint in non-robust control.

5.4.2. Robust voltage control

Fig. 10(b) compares the daily boxplot post-control nodal voltage magnitudes for all the nodes using the robust voltage control. As it can be seen, robust voltage control succeeds in reducing voltage violations. Robust voltage control using estimates from RLS-SF and RLS-DF perform similarly to the model-based controls (i.e., the maximum voltage magnitude is near the upper bound).

Fig. 11 shows the control results for the RLS-DF, comparing model-less robust and non-robust methods against model-based control. Fig. 11(a) shows the voltage of node 15 under different control schemes. It can be observed that model-less robust control keeps the voltage within the imposed upper bound and close to the model-based approach, whereas the non-robust method has higher voltage violations. Fig. 11(b) shows the curtailed PV generation for node 15, and it can be seen that model-less controls curtail more than model-based control. The model-based control curtails 86.5 kWh out of the total 210 kWh PV generation, whereas model-less non-robust and robust schemes curtail 106 and 104 kWh respectively. This is because they compute a more conservative solution to avoid voltage violations. Although the non-robust scheme curtails more, it fails to satisfy the voltage bounds due to inaccurate reactive power actuation. Finally, Fig. 11(c) shows the reactive power injections in three cases. Model-based and robust control follow a similar pattern, whereas non-robust provides less reactive power during the middle of the day.

5.4.3. Performance with measurement noise

We also present a performance comparison when robust or non-robust control is coupled with different estimation techniques for different IT classes of measurement noise. The results are summarised in Table 3 resulting in different and the following observations: (i) non-robust control always results in voltage violations, even when the measurement noise is minimum; in contrast, robust control achieves negligible violations; (ii) RLS-SF and RLS-DF-based robust control performed the best with respect to maximum voltage violations, irrespective of the IT class.

6. Conclusion

This work proposed a model-less robust voltage control scheme accounting for the uncertainty on the sensitivity coefficients which

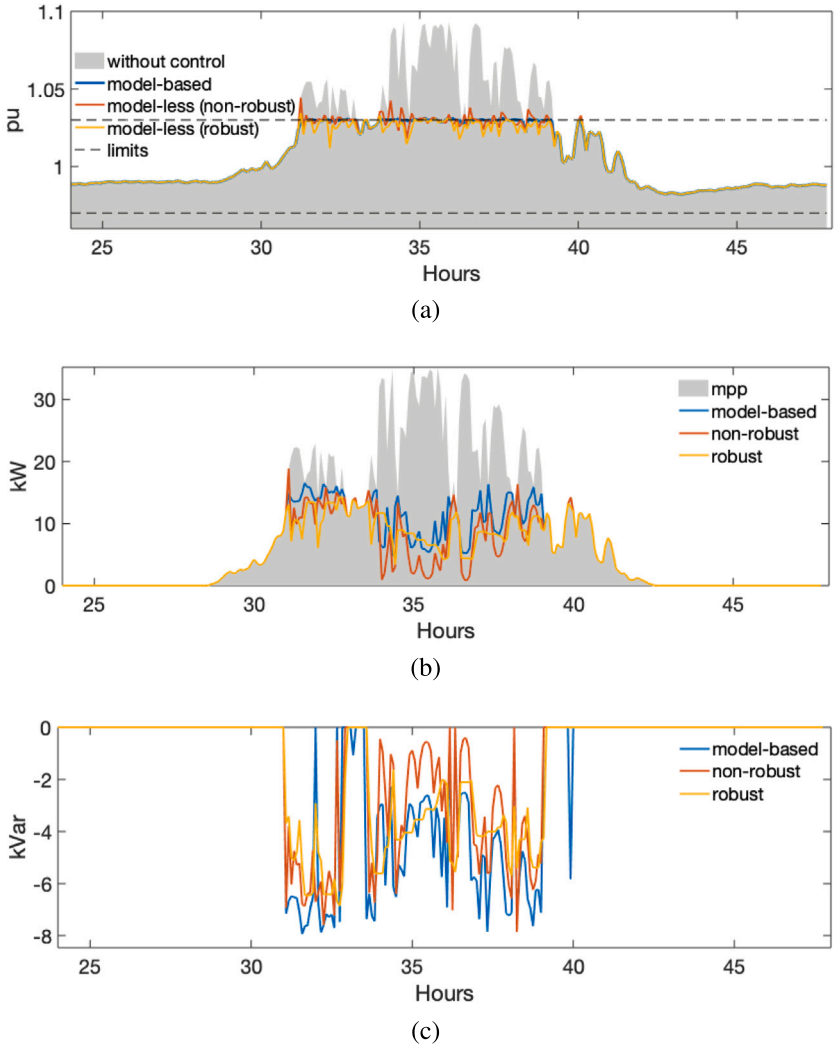

Fig. 11. Control results using RLS-DF for robust, non-robust and model-based controls: (a) voltage magnitude, (b) active power and (c) reactive power for node 15.

are estimated from measurements. The control framework consisted of two stages: in the first, voltage sensitivity coefficients and their uncertainties are estimated using the measurements of nodal voltage magnitudes and active and reactive power. In the second stage, these estimated coefficients and their uncertainties are used by for the robust voltage control problems.

The voltage sensitivity coefficients are estimated using a recursive estimation algorithm, where the LS is solved offline to provide a rough estimate of the coefficient using a large number of historical measurements. Then, RLS is used to refine such a preliminary estimation by using the most recent measurements. The work also compares different forgetting schemes in online RLS estimation. We incorporate the uncertainty of the estimated coefficient to formulate a robust voltage control.

The scheme is validated for controlling active/reactive power injections from distributed PV generation units connected to the CIGRE low-voltage benchmark network. The results show that the non-robust voltage controls fail to satisfy the voltage constraint (i.e., when uncertainty on the estimated coefficients are not accounted for). The proposed robust control scheme respects the voltage control limit even in the highest instrument class. The performance comparison with respect to different estimation schemes shows that an online estimation scheme with directional forgetting performs the best.

CRediT authorship contribution statement

Rahul Gupta: Conceptualization, Methodology, Software, Validation, Visualization, Writing – original draft. **Fabrizio Sossan:** Supervision, Writing – review & editing, Resources. **Mario Paolone:** Supervision, Writing – review & editing, Resources, Project administration.

Declaration of competing interest

The authors declare that they have no known competing financial interests or personal relationships that could have appeared to influence the work reported in this paper.

Acknowledgment

This project is carried out within the frame of the Swiss Centre for Competence in Energy Research on the Future Swiss Electrical Infrastructure (SCCER-FURIES) with the financial support of the Swiss Innovation Agency (Innosuisse - SCCER program).

Appendix. Measurement noise validation

In Eq. (4), the noise $\mathcal{W}$ is assumed to be Gaussian. The noise $\mathcal{W}$ is composed of deviations of the nodal voltage magnitudes and active/reactive power measurements, and are obtained from the voltages

and currents measurements Algorithm 1 as per the ITs' specification (Table 1). We may verify the Gaussian property by looking at the standard quantile–quantile (QQ) plot in Fig. 12. The plot is shown for IT class 0.5. As observed from the plot, the most quantiles (shown in blue dots) follow the standard normal distribution (shown as a straight line). Therefore, the Gaussian assumption in (4) is reasonable.

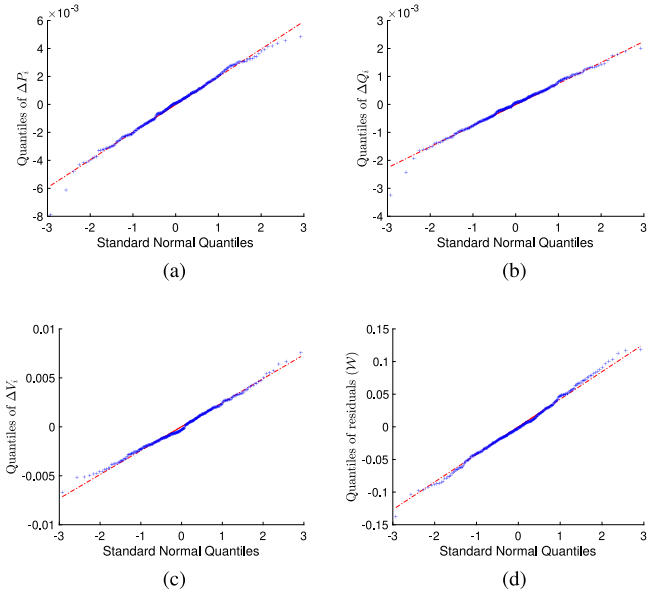

Fig. 12. QQ plot of the deviations of (a) active power, (b) reactive power, (c) voltage magnitudes, and (c) residuals.

References

[1] Power Quality Application Guide, Voltage disturbances, 2004, Standard EN 50160.

[2] CIGRE' Task Force C6.04.02, Benchmark Systems for Network Integration of renewable and Distributed Energy Resources, Tech. Rep., Cigre' International Council on large electric systems, 2009.

[3] IEEE Std 1159-2009, IEEE Recommended Practice for Monitoring Electric Power Quality, Tech. Rep., (Revision of IEEE Std 1159-1995), 2009.

[4] N. Hatziargyriou, J. Amantegui, B. Andersen, M. Armstrong, P. Boss, B. Dalle, G. de Montravel, A. Negri, C.A. Nucci, P. Southwell, CIGRE WG "NEtwork of the Future", 2011.

[5] W. CIGRÉ, C6. 11,"Development and Operation of Active Distribution Networks," Cigré, Paris, Idf, 2011.

[6] F. Pilo, S. Jupe, F. Silvestro, K. El Bakari, C. Abbey, G. Celli, J. Taylor, A. Baitch, C. Carter-Brown, Planning and optimisation of active distribution systems-An overview of CIGRE working group C6. 19 activities, 2012, IET.

[7] K. Christakou, Real-Time Optimal Controls for Active Distribution Networks: from Concepts to Applications (Ph.D. thesis), Ph. D. dissertation, Dept. Information and communications, Univ. École, 2015.

[8] Y.P. Agalgaonkar, B.C. Pal, R.A. Jabr, Distribution voltage control considering the impact of PV generation on tap changers and autonomous regulators, IEEE Trans. Power Syst. 29 (1) (2013) 182–192.

[9] R.K. Gupta, F. Sossan, M. Paolone, Grid-aware distributed model predictive control of heterogeneous resources in a distribution network: Theory and experimental validation, IEEE Trans. Energy Conv. (2020).

[10] H. Su, P. Li, X. Fu, L. Yu, C. Wang, Augmented sensitivity estimation based voltage control strategy of active distribution networks with PMU measurement, IEEE Access 7 (2019) 44987–44997.

[11] M. Carpita, A. Dassatti, M. Bozorg, J. Jaton, S. Reynaud, O. Mousavi, Low voltage grid monitoring and control enhancement: The GridEye solution, in: 2019 ICCEP, IEEE, 2019, pp. 94–99.

[12] E.L. da Silva, A.M.N. Lima, M.B. de Rossiter Corrêa, M.A. Vitorino, L.T. Barbosa, Data-driven sensitivity coefficients estimation for cooperative control of PV inverters, IEEE Trans. Power Deliv. 35 (1) (2019) 278–287.

[13] S. Nowak, Y.C. Chen, L. Wang, Measurement-based optimal DER dispatch with a recursively estimated sensitivity model, IEEE Trans. Power Syst. 35 (6) (2020) 4792–4802.

[14] R.K. Gupta, F. Sossan, J.-Y. Le Boudec, M. Paolone, Compound admittance matrix estimation of three-phase untransposed power distribution grids using synchrophasor measurements, IEEE Trans. Instrum. Meas. 70 (2021) 1–13.

[15] J. Zhang, Z. Wang, X. Zheng, L. Guan, C. Chung, Locally weighted ridge regression for power system online sensitivity identification considering data collinearity, IEEE Trans. Power Syst. 33 (2) (2017) 1624–1634.

[16] J. Zhang, C. Chung, L. Guan, Noise effect and noise-assisted ensemble regression in power system online sensitivity identification, IEEE Trans. Ind. Info. 13 (5) (2017) 2302–2310.

[17] D. Bertsimas, D.B. Brown, C. Caramanis, Theory and applications of robust optimization, SIAM Rev. 53 (3) (2011) 464–501.

[18] T. Söderström, P. Stoica, System Identification, Prentice-Hall International, 1989.

[19] D.L. Mills, Internet time synchronization: The network time protocol, IEEE Trans. Commun. 39 (10) (1991) 1482–1493.

[20] R. Gupta, F. Sossan, M. Paolone, Performance assessment of linearized OPF-based distributed real-time predictive control, in: IEEE PowerTech 2019, Milan, Italy, 2019.

[21] Instrument Transformers:, Additional requirements for electronic voltage transformers, 2011, Standard IEC 61869–8.

[22] Instrument Transformers:, Additional requirements for electronic current transformers, 2014, Standard IEC 61869–7.

[23] J. Parkum, N.K. Poulsen, J. Holst, Recursive forgetting algorithms, Internat. J. Control 55 (1) (1992) 109–128.

[24] A. Vahidi, A. Stefanopoulou, H. Peng, Recursive least squares with forgetting for online estimation of vehicle mass and road grade: theory and experiments, Veh. Syst. Dynam. 43 (1) (2005) 31–55.

[25] T. Fortescue, L.S. Kershenbaum, B.E. Ydstie, Implementation of self-tuning regulators with variable forgetting factors, Automatica 17 (6) (1981) 831–835.

[26] L. Cao, H.M. Schwartz, A novel recursive algorithm for directional forgetting, in: Proceedings of the 1999 American Control Conference (Cat. No. 99CH36251), Vol. 2, IEEE, 1999, pp. 1334–1338.

[27] S. Bittanti, P. Bolzern, M. Campi, Exponential convergence of a modified directional forgetting identification algorithm, Systems Control Lett. 14 (2) (1990) 131–137.

[28] K. Christakou, M. Paolone, A. Abur, Voltage control in active distribution networks under uncertainty in the system model: A robust optimization approach, IEEE Trans. Smart Grid 9 (6) (2017) 5631–5642.

[29] D. Bertsimas, M. Sim, The price of robustness, Oper. Res. 52 (1) (2004) 35–53.

[30] A. Khosravi, S. Nahavandi, D. Creighton, Prediction intervals for short-term wind farm power generation forecasts, IEEE Trans. Sustain. Energy 4 (3) (2013) 602–610.